Sophorolipids: a yeast-derived glycolipid as greener structure directing agents for self-assembled nanomaterials†

Niki Baccile,*[a] Nadine Nassif,[a] Luca Malfatti,[a,b] Inge N. A. Van Bogaert,[c] Wim Soetaert,[c] Gerard Pehau-Arnaudet[d] and Florence Babonneau[a]

Received 1st June 2010, Accepted 30th June 2010
DOI: 10.1039/c0gc00163e

Sophorolipids, fully natural glycolipids, can form in water nanometre-size micelles of various geometries depending on their concentration as shown by small angle neutron scattering experiments. This property allows use of them, for the first time, as structure directing agents in the synthesis of nanostructured silica thin films *via* the evaporation induced self-assembly (EISA) process.

Introduction

Alkylglycosides are a class of natural non-toxic surfactants whose properties have been largely studied and their commercial development is well-established.[1] Nevertheless, these industrially-produced compounds are generally synthesized by a multitude of chemical steps which limit the ideal "full green" approach suitable in the perspective of material synthesis *via* the sol–gel process.[2] For this reason, we turned our interest towards sophorolipids (SL), microbe-synthesized alkylglycosides (Scheme 1), as structure-directing agents for mesoporous silica obtained *via* the sol–gel process using the well-established evaporation induced self-assembly (EISA)[3] technique for thin film synthesis. Mesoporous materials have aroused a growing interest because of their tunable and narrow pore size distribution and extremely high specific surface area.[4] These peculiarities make them ideal functionalizable materials for many applications such as sensing,[5] photovoltaic electrodes,[6] filtration[7] and catalysis.[8] So far, these materials are almost exclusively made with synthetic surfactants employed as structure directing agents and which raise important questions about sustainability and toxicity.

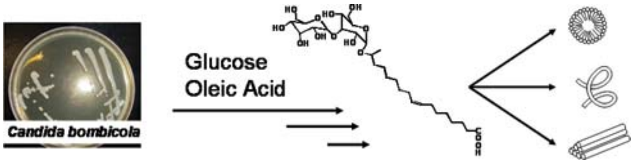

Scheme 1 Sophorolipids are commonly obtained from the culture broth of the yeast *Candida bombicola*. The acidic form of SL used in this work is obtained after processing the sophorose mixture (see experimental in the ESI†).

If compared to many other surfactants, SL are entirely obtained from renewable agroresources (rapeseed oil, oleic acid, carbohydrates) through a robust microbial synthesis with abundant production rates (up to 300–400 g L^{-1});[9] for this reason, they have mainly attracted the attention of the cleansing industry (they can be found in Ecover© biobased products) even if recent studies showed the existence of interesting supramolecular assemblies.[9c] Their synthesis conditions, sources and applications have been recently reviewed by Van Bogaert *et al.*[10] Despite the potential interest for these compounds in dermatology[11] and health care[12] (more than 40 patents have been deposited on their synthesis and applications[13]), their self-assembly properties in solution have only been partially explored[9c] and their behaviour at the mesoscale level is still largely unknown. So far, they have never been used as structure directing agents.

In this work, the acidic form of sophorolipid molecule (simply referred to as SL), as shown in Scheme 1, is synthesized from glucose and oleic acid substrates using the yeast *Candida bombicola* (see experimental in the ESI†). We show here that, in water, such molecules can form micellar aggregates of various shapes depending on their concentration and thus can be successfully exploited as structure-directing agents (SDA) for the synthesis of nanostructured silica thin films.[14]

Results and discussion

Self-assembly of SL

Considering that very little is known about the self-assembling behavior of SL in water, we decided to investigate this point by mean of small angle neutron scattering (SANS) experiments performed on the SL in D_2O. Knowledge of the optimal self-assembling conditions of SL is of paramount importance for their best employment in the synthesis of mesostructured silica thin films, as shown later.

SANS is an extremely powerful technique which is generally used to study the shapes, size, volumes and specific surface

---

[a] *UPMC Univ Paris 6, CNRS-UMR 7574, Chimie de la Matière Condensée de Paris, Collège de France, 11 place Marcellin Berthelot, 75005, Paris, France. E-mail: niki.baccile@upmc.fr; Fax: +33-1-44271504; Tel: +33-144271544*
[b] *Laboratorio di Scienza dei Materiali e Nanotecnologie (LMNT) and CR-INSTM, D.A.P., Università di Sassari, Palazzo Pou Salid, Piazza Duomo 6, 07041, Alghero (Sassari), Italy*
[c] *InBio, Department of Biochemical and Microbial Technology, Faculty of Bioscience Engineering, Ghent University, Coupure Links 653, 9000, Ghent, Belgium*
[d] *URA 2185, Institut Pasteur, 28 Rue du Docteur Roux, 75015, Paris, France*

† Electronic Supplementary Information (ESI) available: Experimental conditions: synthesis of SL, synthesis of silica film by EISA, small-angle X-ray scattering, small angle neutron scattering. Fig. S1: fit of SANS curves. Fig. S2: transmission electron microscopy experiments under cryogenic conditions. See DOI: 10.1039/c0gc00163e/

areas of colloids in general and surfactant-derived micelles in particular. According to SANS theory (see ESI†), the main contributions to the intensity $I(q)$ come from the volume of the objects, their volumetric fraction, the contrast with the solvent, the form factor (related to the geometry of one scatterer) and their structure factor (related to their organization in space). In general, at low concentration values (independent objects with no mutual interactions), one can assume that the structure factor is equal to 1 and the form factor alone (well-known for simple objects like spheres, cylinders, *etc.*) can be fitted to retrieve information on the shape of the micelle and its dimensions. In alternative, one can look more closely at the different parts of the SANS data set: (1) the low-q part of the curve gives some insights on the overall size (Guinier regime) and the geometrical features of the micellar object by looking at the slope (0, −1, −2 respectively for spheres, cylinders, disks); (2) the high-q region (Porod regime) is, on the contrary, more sensitive to the type of solvent/colloid interface (smooth, as in spheres, or fractal, as in polymer brushes) and to its dimension (cross-section).

Fig. 1 shows the variation of the absolute scattered intensity normalized by the concentration, $I(q)/c$, at different SL weight percentage concentrations prepared at their equilibrium pH (~4.5). As a general comment, we can say that the typical $\log(I)$ *vs.* $\log(q)$ plot representation of SANS data indicates the existence of micellar objects of different geometries, as represented on the Fig. 1 itself. Low-q: the slope variation shows an evolution in the shape of the micelles as a function of concentration, as schematically represented in the inset of Fig. 1. Interestingly, no specific correlation peak is observed, as one would expect at high concentration values; we will come back to this point later on in the discussion. High-q: superposition of the spectra in this region shows that the cross-sectional dimension of the micellar objects does not consistently vary with concentration, as previously observed in similar glycolipid systems.[15] A more detailed analysis follows.

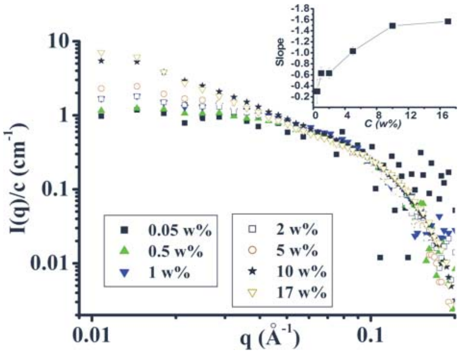

Fig. 1 (a) SANS curves of SL in D_2O at variable concentrations and at SL equilibrium pH (~4.5). $I(q)$, given in absolute scale (cm^{-1}), is scaled by the wt% concentration of the SL in solution. Inset: schematic evolution of slopes in (a) for $0.015 < q < 0.04$.

SL concentration <1 wt%. In this regime, micelles can be considered as non-interacting monodispersed objects, whose form factor can be fitted with a spherical particle model (see Fig. S1, ESI†), which results in objects with a radius, $R = 2.8 \pm 0.2$ nm, as further confirmed by Cryo-TEM experiments (Fig. S2A, ESI†). The micellar radius can also be estimated from the radius of gyration, R_G, obtained from the Guinier plot, $\ln(I(q))$ *vs.* q^2 (see eqn S1, ESI†) at low-q. This approach is based on the following two assumptions: the inter-micellar interaction is minimal, and the contribution to SANS intensity from large aggregates in the q region under interest is negligible ($qR < 1$). These hypothesis are verified here for $q < 0.04$ Å^{-1}. At $c = 0.5$ wt%, $R = 3.1 \pm 0.3$ nm which is consistent with the value obtained above. Very interestingly, these values are also fully consistent with the $R = 2.5$ nm, which was obtained by Gross *et al.*[9c] after dynamic light scattering (DLS) measurements, which, on the contrary, do not provide the exact micellar geometry. From the analysis of the $I(q)q^4$ values at high-q (Porod regime, eqn S2, ESI†), some complementary information can be obtained about the total surface area per unit volume, S_V, exhibited by the micelles. A simple calculation gives an estimated $S_V = 600 \pm 50$ m^2 cm^{-3} and an aggregation number of about 50 SL molecules per micelle, if one estimates the volume per molecule to about 950 Å^3.‡ Despite the lack of information about the exact configuration of the SL molecule in solution and, consequently, its real volume, these values appear to be self-consistent and coherent with an homogenous distribution of about 5×10^{18} SL molecules per cm^3 (at $c = 0.0048$ g cm^{-3}) into spherical micelles having an average radius of 3.0 nm.

SL concentration ≥ 1 wt%. In this regime, the slope at low-q (Fig. 1) increases and micelles are no-longer spherical. At $c = 5$ wt%, a cylindrical model can be used to fit the form factor (see Fig. S1). Typical values for the cross-sectional radius are 1.6 ± 0.3 nm. At $c \geq 10$ wt%, the slope at low-q increases up to −1.6 (inset in Fig. 1). These data show that the attribution of a defined shape is here an harsh task and a more appropriate model accounting for the whole q-range should probably be employed, as reported in typical SANS studies for similar systems.[15] Nevertheless, even if the aggregation behaviour of SL has never been studied before, many studies exist for similar alkyl-glucosidic systems. For instance, Zhang *et al.*[15] report on the study of *n*-alkyl-*b*-D-glucopyranosides in water, Milkereit *et al.*[16] have studied oleic oil based glyco-surfactants and Dahrazma *et al.*[17] studied the micellization of rhamnolipids as a function of pH. If we compare our data to these and other similar studies,[15a,18] we find a fairly good correlation between the SANS behaviour both in the high-q and low-q regions. In general, alkylglucoside surfactants have the tendency to form both spherical and cylindrical objects according to the specific head-to-tail geometry, the concentration, c, in solution and the presence of a co-solvent. In our case, micelles are spherical at low c while they start to elongate from $c > 0.5$ wt%. Isolated rigid rods would provide a −1 slope, while slopes between −1 and −2, as it is the case here, have been reported for long flexible cylindrical micelles.[15,16] Such a detailed analysis is extremely important for the better understanding of the self-assembly properties of SL in solution as it completes the previous study from Gross *et al.*;[9c] in fact, authors reported on the formation of both micellar and micrometre-sized supra-molecular assemblies as a function of pH and concentration. Despite the small angle X-ray scattering (SAXS) and DLS analysis, no clear-cut answer could be provided on the shape of the micelles. Further proof of the cylindrical shape of the micelles is provided here by cryo-TEM experiments shown in Fig. S2 B,C. (ESI†)

Mesoporous thin film synthesis from SL

The information obtained from the SANS study can be exploited in the synthesis of mesoporous thin films *via* the EISA process,[3] where SL are used as a template. These experiments have been performed at $c = 10$ wt%, which combines a good wettability of the film and which should provide flexible cylindrical micellar aggregates.

Fig. 2-a shows the typical SAXS pattern of a SL-templated film. The presence of a broad peak at $q = 0.13$ Å^{-1} ($d = 4.83$ nm) indicates the existence of a porous network typical for a wormlike structure, as confirmed by transmission electron microscopy (TEM) in Fig. 2b. Interestingly, such an arrangement of the pores is consistent with SANS measurements shown earlier and which suggested the presence of long cylindrical flexible micelles. The repeatability of the experiment has been tested several times without significant changes in the pore arrangement. TEM image (Fig. 2b) shows a pore diameter of 2.4 ± 0.2 nm, which is a value coherent with the interporous distance measured by SAXS. We actually found that the porous morphology and dimension can be tuned by changing the pH of the SL solution. In fact, the SL molecule contains a COOH group at the end of the hydrocarbon chain and which provides a pH-responsive probe. Fig. 2c,d compares TEM micrographs of the mesoporous thin film prepared from two solutions stabilized at an acidic ($2 < pH < 3$) and a neutral pH ($pH = 6.5$). When pH is raised close to neutrality (Fig. 2-d), a more elongated porous geometry can be observed. In fact the mesostructure seems to be composed by stacks of disk-like pores having an average length of ≈25 nm and an estimated thickness of 4.5 ± 0.8 nm.

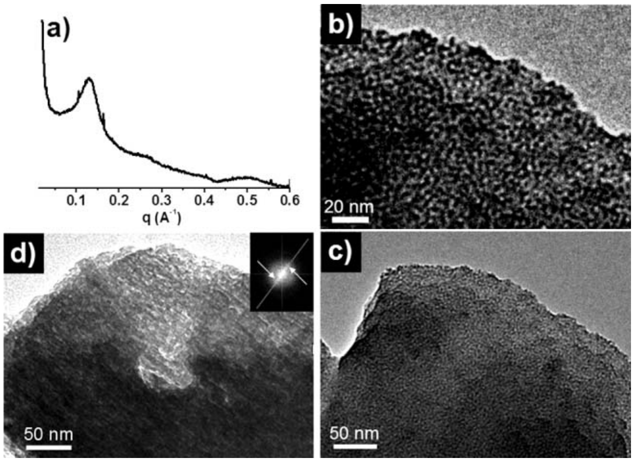

Fig. 2 SAXS pattern (a) and TEM images (b, c) of a 10 wt% SL-templated dip-coated mesoporous silica film. (d) TEM image of a 10 wt% SL-templated porous silica film obtained at from a neutral-pH solution (pH = 6.5). Both films are calcined at 350 °C for 1 h before measurements.

Such a particular pore organization is also confirmed by the Fourier transform of the image as shown in the inset of Fig. 2d. This analysis reveals the presence of an anisotropic signal which is due to a coherent alignment of the pores. The strong influence of pH on the self-assembling behaviour of SL in water is also confirmed by SANS experiments, as shown in Fig. 3. At pH = 6.5, where COO^{-} species should be predominant, and for concentration values $c \geq 2$ wt%, an interaction peak centered at $q = 0.06$ Å^{-1} (about 10 nm) dominates the SANS signal. This shows that micellar objects are now regularly spaced and their interaction is strong. Further experiments are on-going to clarify the influence of pH on the self-assembly properties and on the morphology of the porous structure.

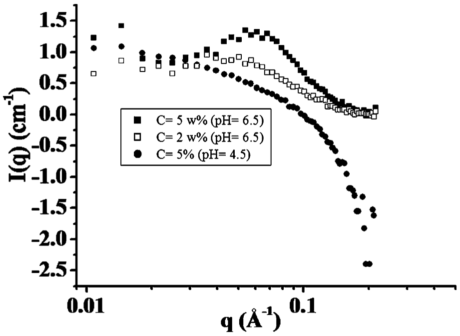

Fig. 3 (a) SANS experiments performed on SL/D_2O solutions ($c = 2$ and 5 wt%). To enhance the interaction peak, curves are represented in a lin-log scale. For comparison, the experiment performed on a pH = 4.5 ($c = 5$ wt%, same as in Fig. 1) solution is reported in a usual log-log scale.

Conclusion

In conclusion, we show here a direct application of sophorolipids, a microbially-produced and bio-engineerable glycolipid, in the synthesis of mesostructured silica thin films. Sophorolipids are able to form pH-responsive nanometre-sized micelles with spherical and worm-like shapes in water as a function of their concentration and they reveal to be suitable alternatives to common petrochemical surfactants in the structure-directing agent process of inorganic materials.

Acknowledgements

We kindly acknowledge Prof. Walter Richtering (RWTH Aachen University, Germany), Jose Teixeira (LLB, CEA/CNRS, France), Marianne Impéror-Clerc (LPS, Université d'Orsay, France) and François Ribot (LCMCP, Université Pierre et Marie Curie, Paris, France) for helpful discussions on SANS studies. We are also thankful to the Industrial Yeast Collection, DBVPG (University of Perugia, Italy) for providing us the yeast *Candida bombicola* and their technical support. Gervaise Mosser (LCMCP, Université Pierre et Marie Curie, Paris, France) is kindly acknowledged for help in cryo-TEM experiments.

References

‡ Calculation of S_V and aggregation number. S_V is readily calculated from the $I(q)q^4$ plot from eqn S2, while the aggregation number can be estimated from S_V, the micellar radius obtained from the Guinier analysis, the density of the SL (=1.092 g cm^{-3}), the atomic weight of the acidic SL (622 g mol^{-1}) and the irradiated volume (0.98 cm^3, considering a 0.2 cm quartz cell, where the beamsize is 0.7 × 0.7 cm). The volume of one SL molecule (950 Å^3) is estimated from its density and molecular weight.

1 W. von Rybinski and K. Hill, *Angew. Chem., Int. Ed.*, 1998, **37**, 1328–1345.
2 N. Baccile, F. Babonneau, B. Thomas and T. Coradin, *J. Mater. Chem.*, 2009, **19**, 8537–8559.

3 C. J. Brinker, Y. Lu, A. Sellinger and H. Fan, *Adv. Mater.*, 1999, **11**, 579–585.

4 G. J. A. A. Soler-Illia, C. Sanchez, B. Lebeau and J. Patarin, *Chem. Rev.*, 2002, **102**, 4093–4138.

5 (*a*) A. Bearzotti, P. Innocenzi, P. Falcaro, J. Mio Bertolo and E. Traversa, *Sens. Actuators, B*, 2003, **95**, 107–110; (*b*) L. Nicole, C. Boissière, D. Grosso, P. Hesemann, J. Moreaub and Clément Sanchez, *Chem. Commun.*, 2004, 2312–2313.

6 (*a*) L. Malfatti, P. Falcaro, H. Amenitsch, S. Caramori, R. Argazzi, C. A. Bignozzi, S. Enzo, M. Maggini, P. Innocenzi and Microporous, *Microporous Mesoporous Mater.*, 2006, **88**, 304–311; (*b*) E. Lancelle-Beltran, P. Prené, C. Boscher, P. Belleville, P. Buvat, S: Lambert, F. Guillet, C. Boissière, D. Grosso and C. Sanchez, *Chem. Mater.*, 2006, **18**, 6152–6156.

7 N. Baccile and F. Babonneau, *Microporous Mesoporous Mater.*, 2008, **110**, 534–542.

8 A. Corma, *Chem. Rev.*, 1997, **97**, 2373.

9 (*a*) U. Rau, S. Hammen, R. Heckmann, V. Wray and S. Lang, *Ind. Crops Prod.*, 2001, **13**, 85–92; (*b*) A. P. Tulloch, A. Hill and J. F. T. Spencer, *Can. J. Chem.*, 1968, **46**, 3337–3351; (*c*) S. Zhou, C. Xu, J. Wang, W. Gao, R. Akhverdiyeva, V. Shah and R. Gross, *Langmuir*, 2004, **20**, 7926–7932; (*d*) H.-J. Asmer, S. Lang, F. Wagner and V. Wray, *J. Am. Oil Chem. Soc.*, 1988, **65**, 1460–1466.

10 I. N. A. Van Bogaert, K. Saerens, C. De Muynck, D. Develter, W. Soetaert and E. J. Vandamme, *Appl. Microbiol. Biotechnol.*, 2007, **76**, 23–34.

11 M. Maingault, Use of sophorolipids and cosmetic and dermatological compositions, WO/1995/034282A.

12 S. L. Fu, S. R. Wallner, W. B. Bowne, M. D. Hagler, M. E. Zenilman, R. Gross and M. H. Bluth, *J. Surg. Res.*, 2008, **148**, 77–82.

13 A. M. Shete, G. Wadhawa, I. M. Banat and B. A. Chopade, *J. Sci. Ind. Res.*, 2006, **65**, 91–115.

14 (*a*) P. Yang, D. Zhao, D. I. Margolese, B. F. Chmelka and G. D. Stucky, *Nature*, 1998, **396**, 152–155; (*b*) L. Nicole, C. Boissière, D. Grosso, A. Quach and C. Sanchez, *J. Mater. Chem.*, 2005, **15**, 3598–3627; (*c*) P. Innocenzi, L. Malfatti, T. Kidchob and P. Falcaro, *Chem. Mater.*, 2009, **21**, 2555–2564.

15 (*a*) A. Stradner, O. Glatter and P. Schurtenberger, *Langmuir*, 2000, **16**, 5354–5364; (*b*) R. Zhang, P. A. Marone, P. Thiyagarajan and D. M. Tiede, *Langmuir*, 1999, **15**, 7510–7519.

16 G. Milkereit, V. M. Garamus, K. Veermans, R. Willumeit and V. Vill, *J. Colloid Interface Sci.*, 2005, **284**, 704–713.

17 B Dahrazma, C. N. Mulligan and M.-P. Nieh, *J. Colloid Interface Sci.*, 2008, **319**, 590–593.

18 B. Hoffmann and G. Platz, *Curr. Opin. Colloid Interface Sci.*, 2001, **6**, 171–177.